













Article

Inter- and Intraspecific Venom Variation in the Reclusive Rear-Fanged Black-Striped Snakes (*Coniophanes*)

John Henry Fowler ^{1,*}, Ramses Alejandro Rosales-García ¹, Rhett M. Rautsaw ¹, Michael P. Hogan ^{2,3},
Erich P. Hofmann ^{1,4}, Andrew J. Mason ^{1,5}, Ramon Nagesan ³, Miguel Borja ⁶, Luis Herrera ⁷,
Gamaliel Castañeda-Gaytan ⁶, Alison R. Davis Rabosky ³, Darin R. Rokyta ² and Christopher L. Parkinson ^{1,*}

¹ Department of Biological Sciences, Clemson University, Clemson, SC 29634, USA; ramsesr@g.clemson.edu (R.A.R.-G.)

² Department of Biological Science, Florida State University, Tallahassee, FL 32306, USA

³ Department of Ecology and Evolutionary Biology and Museum of Zoology (UMMZ), University of Michigan, Ann Arbor, MI 48109, USA

⁴ Science Department, Cape Fear Community College, Wilmington, NC 28401, USA

⁵ Department of Evolution, Ecology and Organismal Biology, The Ohio State University, Columbus, OH 43210, USA

⁶ Facultad de Ciencias Biológicas, Universidad Juárez del Estado de Durango, Gómez Palacio 35010, Durango, Mexico; gamaliel.cg@gmail.com (G.C.-G.)

⁷ Instituto de Investigación en Ciencias Biológicas y Ambientales de Honduras, Facultad de Ciencias, Universidad Nacional Autónoma de Honduras, San Pedro Sula 21102, Honduras; laherrera@unah.edu.hn

* Correspondence: johnhen@g.clemson.edu (J.H.F.); viper@clemson.edu (C.L.P.)

Abstract

Our current understanding of snake venom is highly biased towards species known to be medically significant in human envenomations. This vastly under-represents the true evolutionary and ecological breadth of snake venom, with gaps spanning entire clades and unique lifestyles. As a result, many genera of rear-fanged snakes lack well-understood venom profiles despite these taxa composing around 65% of known extant snake species. Methodological challenges associated with venom extraction have long been a key reason responsible for the lack of venom research on this group. Modern advancements in venomomics technologies have allowed researchers to overcome many of these challenges and investigate the venom components of understudied genera. The genus *Coniophanes* (black-striped snakes) presents an ideal system for investigating venom and the venom delivery system in a rear-fanged venomous species with well-documented accounts of human envenomations. We sequenced and annotated de novo transcriptomes of the Duvernoy's gland (DVG) for seven individuals across four species of *Coniophanes* (Dipsadidae) and confirmed toxin expression in representative venom proteomes. We assessed interspecific venom variation within this genus and further examined intraspecific venom variation within *C. imperialis*. We found that toxins account for 38.8% to 66% of the total DVG transcriptomes and that 18 toxin families are represented in this genus, with prominent expression of cysteine-rich secretory proteins (CRiSPs) in three species and snake venom metalloproteinases (SVMPs) in all four species. In addition, we used diffusible iodine-based contrast-enhanced computed tomography (diceCT) to better understand the venom delivery system for *C. fissidens*, a widespread species within this genus, showcasing enlarged, grooved, rear fangs in close proximity to a prominent DVG. We provide the first ever characterization of the venom profiles of *Coniophanes*, highlight venom variation between and within species, and outline the venom delivery system of this understudied genus.

Keywords: black-striped snake; *Coniophanes*; rear-fanged snake; snake venom; Duvernoy's gland



Received: 22 January 2026

Revised: 10 February 2026

Accepted: 17 February 2026

Published: 20 February 2026

Copyright: © 2026 by the authors.

Licensee MDPI, Basel, Switzerland.

This article is an open access article distributed under the terms and conditions of the [Creative Commons Attribution \(CC BY\) license](https://creativecommons.org/licenses/by/4.0/).

Key Contribution: This research provides an extensive characterization of the venom components and venom delivery system of *Coniophanes*, a genus of rear-fanged Dipsadid snakes.

1. Introduction

Venom is a complex, medically relevant trait vital for feeding and defense in venomous snakes. Venom responds to selective pressures, evolves rapidly, and can vary ontogenetically, intraspecifically, and interspecifically [1–4]. Venom variation is closely linked to ecological pressures, such as diet [5–8]; as a result, venom is an ideal system for studying gene evolution and the phenotypic response to selection. Snake venom is made up of many different proteins and peptides that are grouped into enzymatic and non-enzymatic toxin families. These families arise and diversify through genetic mechanisms such as duplication, deletion, and neofunctionalization [9–12]. Prominent toxin families include three-finger toxins (3FTx), phospholipase A2s (PLA2s), lectins, snake venom metalloproteinases (SVMPs), and cystine-rich secretory proteins (CRiSPs) [11,13]. The rapid evolutionary potential of venom genes and the homologous nature of these genes across phylogenies make them an ideal system for studying the evolutionary forces driving venom diversity and the extent of venom variation within snakes.

Venomous snakes deliver their toxins using either front-fanged or rear-fanged delivery systems. Front-fanged snakes utilize mobile (solenoglyphous) or fixed (proteroglyphous) fangs paired with a high-pressure venom gland, while rear-fanged (opisthoglyphous) snakes possess enlarged and often grooved rear maxillary teeth paired with a low-pressure Duvernoy’s gland (DVG) [11,14–19]. Most venom research has focused on front-fanged snakes, such as vipers and elapids, which are responsible for nearly all lethal snakebites worldwide [13,20]. Rear-fanged snakes are consistently overlooked in these studies despite composing the majority of extant snake species [18,21]. These snakes possess many venom genes that are homologous to their front-fanged counterparts, and research on their venoms is necessary to form a holistic understanding of snake venom variation and evolution on a phylogeny-wide basis [11]. As a result of their venom delivery system, extracting large venom yields from rear-fanged snakes can be much more challenging than that of vipers or elapids, which has contributed to a lack of research on these species [18]. However, advancements in omics (transcriptomics, proteomics, and genomics) technologies requiring little RNA or DNA input and new venom extraction methodologies have led to rear-fanged snakes receiving more attention from venom researchers [6,11,22–24]. Unsurprisingly, these advancements have led to the discovery of entirely new toxin families, such as snake venom matrix metalloproteinases (svMMPs), lactadherins, and snake venom acid lipases (svLIPAs) found only in rear-fanged snakes [25–29].

Discovering new toxin families and novel venom components spurs new interest in understanding the full scope of venom evolution across snake diversity [30]. Entire genera of rear-fanged snakes possess undescribed venom profiles, including snakes known to cause medically-significant human envenomations [31]. The family Dipsadidae is of special interest as it is the most speciose family of snakes found in the Neotropics with more than 700 species [23], comprising around 20% of all extant snake diversity [24]. Encompassing the majority of colubroid biodiversity within the Neotropics, dipsadids are responsible for a high number of medically relevant bites reported in epidemiological studies in South America [32]. Despite reports from dipsadid bites including examples of paralysis (*Hydrodynastes gigas*), permanent disfigurement (*H. gigas*), and even death (*Phylodryas olfersii*) [32], these snakes are often misclassified as “harmless” [19]. The phylogenetic

abundance, medical relevance, and lack of extensive venom research warrants further investigation into the Dipsadidae family.

Coniophanes, or black-striped snakes, is a genus of small- to medium-sized, rear-fanged, New World, colubroid snakes within the family Dipsadidae. *Coniophanes* is distributed from northern South America, through Central America, and into southern Texas (Figure 1). They typically inhabit humid or subhumid forested regions [33]. The diet of *Coniophanes* appears to primarily consist of anurans, lizards, and insects, along with occasional small snakes and eggs [34–36]. However, at least one species, *C. fissidens*, exhibits a highly generalist diet made up of frogs (including members of the poisonous Dendrobatidae family), lizards, salamanders, snakes (including conspecifics), reptile and amphibian eggs, and invertebrates [34,37–39]. The fangs of *Coniophanes* have been described as two enlarged posterior teeth with grooves, presumably sitting near the Duvernoy’s gland and thus facilitating envenomation. The venom delivery system in *Coniophanes* has not been thoroughly investigated, and *Coniophanes* venom has never been extensively characterized, whether transcriptomic or proteomic, despite researchers possessing evidence of their venom for at least 87 years [40–42]. Bites from the genus *Coniophanes* have been documented to produce burning, itching, numbness, swelling, and redness, and they have been described as producing general effects similar to a bee sting [42,43]. In addition, an author of this manuscript received a bite from a *C. imperialis* on the distal portion of the middle finger that produced painful swelling and erythma, as well as numbness of the finger pads that has persisted for more than a decade (Pers. obs, Hofmann).

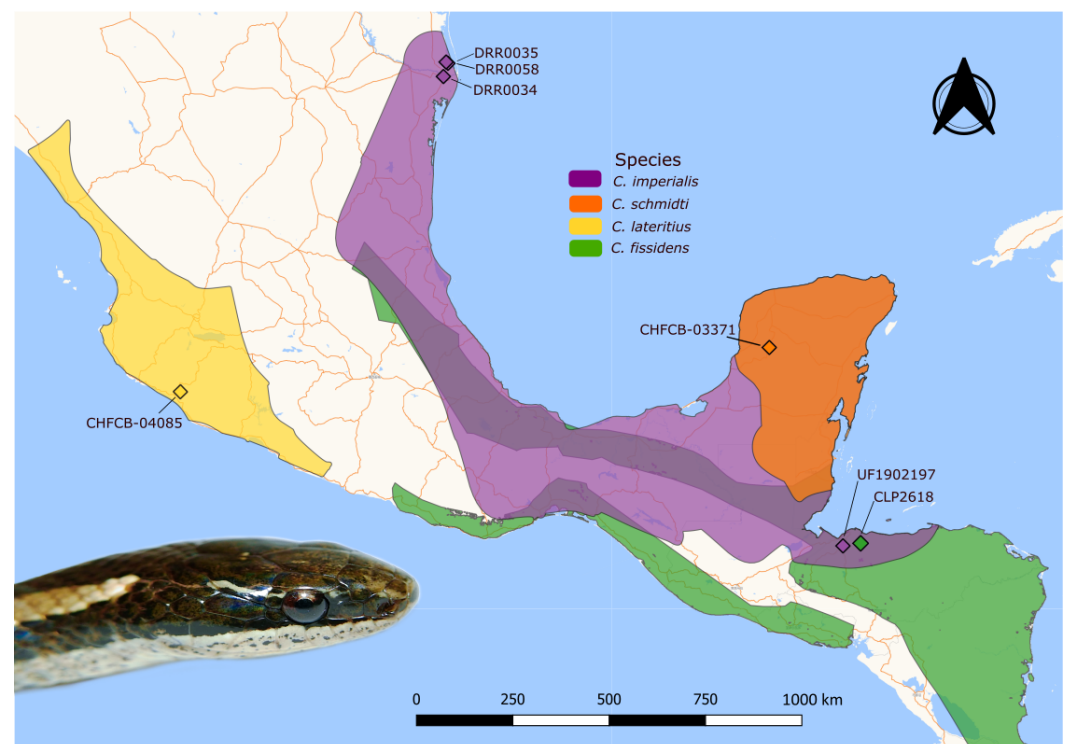


Figure 1. Map of the distributions of the four *Coniophanes* species investigated in this study. Collection localities marked with diamonds. IUCN Red List of Threatened Species (Version 2023-1) distribution ranges were polished with GBIF occurrence data to produce updated distributions. Note that we collected a specimen of *C. imperialis* and a specimen of *C. fissidens* from a location where the ranges of these two species overlap. *C. imperialis* pictured in the photo.

In this study, we use RNA sequencing data to identify the venom components of seven individual snakes across four species from the genus *Coniophanes* spread out from southern Texas to Honduras. We then use differential expression analyses to investigate the venom

profiles within *C. imperialis* from two localities and further verify these findings using proteomics data. In addition, we use diffusible iodine-based contrast-enhanced computed tomography (diceCT) to visualize the venom delivery system of *C. fissidens*. Overall, we generate and characterize the DVG transcriptomes of four species of *Coniophanes*, assess the venom delivery mechanism, and further investigate intraspecific variation in one widespread species using differential expression analyses and qMS proteomic analyses.

2. Results

We sequenced and annotated the transcriptomes for seven individuals of *Coniophanes* across four species, generating between nine and fourteen million assembled reads per sample. In total, 18 toxin families were represented within this genus, and the number of unique toxin transcripts varied from 16 in *C. schmidtii* to 56 in an individual of *C. imperialis* (Table 1).

2.1. Venom Delivery System

By utilizing diffusible iodine-based contrast-enhanced computed tomography (diceCT), we investigated the venom delivery system of a *Coniophanes fissidens* specimen (UMMZ Herps 87643) collected from Chiapas, Mexico. We found that the examined *C. fissidens* clearly displayed large glands in the rear of the mouth and enlarged maxillary teeth with deep longitudinal grooves on the anterior surface (Figure 2).

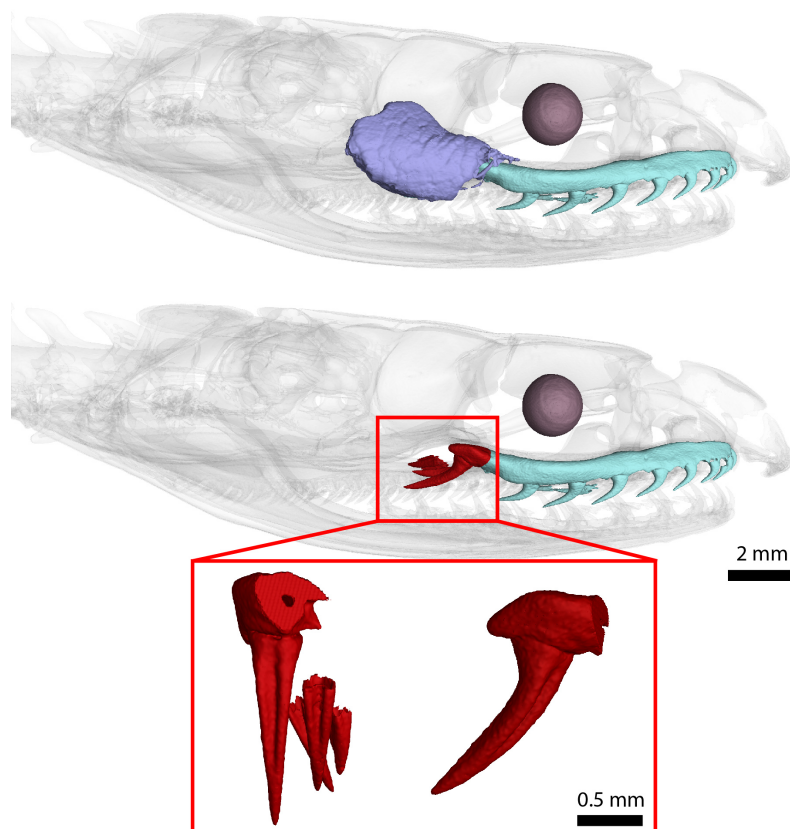


Figure 2. DiceCT scan of *Coniophanes fissidens* (UMMZ Herps 87643) skull. Top picture illustrates the Duvernoy's gland size and location. Bottom picture depicts the enlarged rear fangs of this specimen. Inset highlights the grooved rear fangs including “backup” dentition. Specimen collected from Chiapas, Mexico.

Table 1. Informational table for the *Coniophanes* individuals used in this study. SVL: Snout–vent length.

Species	ID #	Country	SVL (cm)	Weight (g)	Sex	# of Assembled Reads	# of Toxin Transcripts	GenBank Numbers
<i>C. fissidens</i>	CLP2618	Honduras	32	-	Female	9,962,139	27	SRR36021070
<i>C. lateritius</i>	CHFCB-0337	Mexico	33.9	10	Female	9,426,447	24	SRR36021069
<i>C. schmidtii</i>	CHFCB-0408	Mexico	-	14	-	9,579,851	16	SRR36021068
<i>C. imperialis</i>	UF190219	Honduras	30	-	-	10,313,834	56	SRR36021067
<i>C. imperialis</i>	DRR0034	United States	27.5	15	Male	13,379,588	52	SRR36021066
<i>C. imperialis</i>	DRR0035	United States	34	19	Female	13,817,101	50	SRR36021065
<i>C. imperialis</i>	DRR0058	United States	22	5	Female	11,965,322	50	SRR36021064

2.2. Interspecific Toxin Expression

2.2.1. *Coniophanes imperialis*

The consensus average *C. imperialis* transcriptome of four individuals contained 15 toxin families, constituting 41.2% of the transcripts per million (TPM) of the total DVG transcriptome expression. The most highly expressed toxin families were CRiSPs (30.1%), followed by CTLs (23.5%) and 3FTx (20.4%) of the total toxin TPM (Figure 3).

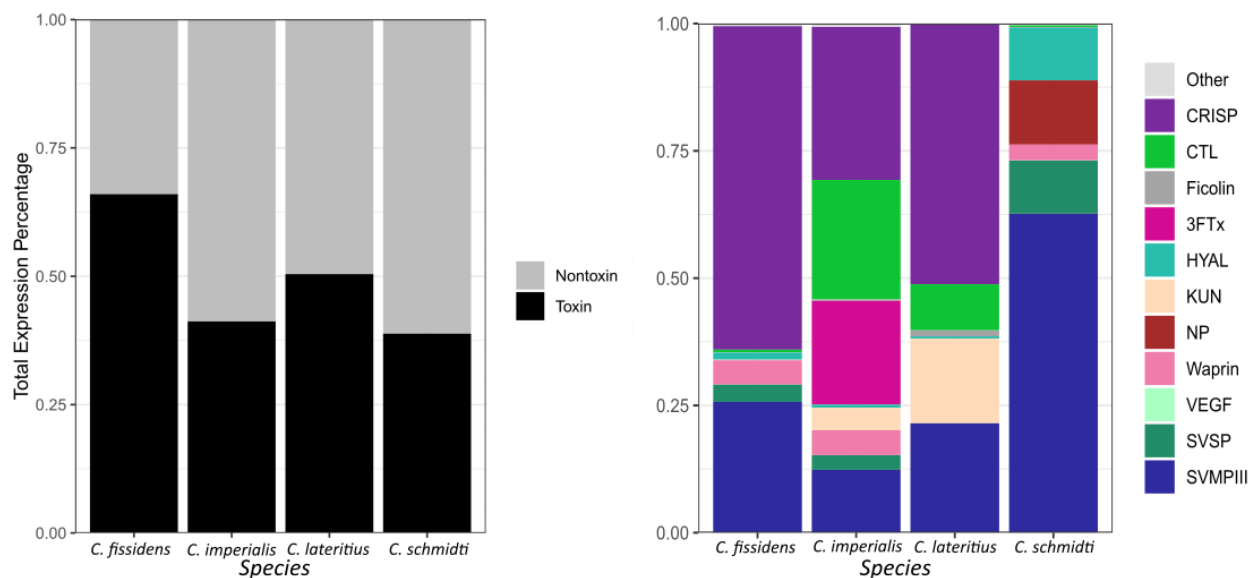


Figure 3. Venom transcriptome characterization of four species of *Coniophanes*. Transcriptomes for *C. fissidens*, *C. lateritius*, and *C. schmidtii* are representative of a single individual each. *C. imperialis* displays average toxin expression across the four individuals of this species. **(Left)** The toxin and nontoxin transcripts per million (TPM) percentage for all four species. **(Right)** The TPM percentage of toxin families from total toxin expression for all four species. Specific epithets of the four species on the x-axis. Color legend on the right indicates toxin families. Figure presenting all toxin families expressed in the transcriptomes can be found in Figure S1 (see Supplementary Materials). [CRiSP: cystine-rich secretory proteins, CTL: C-type lectins, 3FTx: three-finger toxins, HYAL: hyaluronidase, KUN: Kunitz-type proteins, NP: natriuretic peptides, VEGF: vascular endothelial growth factor, SVSP: snake venom serine proteases, SVMPIII: PIII snake venom metalloproteinases].

2.2.2. *Coniophanes fissidens*

The *C. fissidens* transcriptome contained 13 toxin families composing 66% of the TPM within the total DVG transcriptome. Of the toxins, the most highly expressed toxin family was CRiSPs (63.6%), followed by SVMPIIIs (25.7%) (Figure 3).

2.2.3. *Coniophanes lateritius*

The *C. lateritius* transcriptome contained 13 toxin families accounting for 50.4% of the TPM within the total DVG transcriptome. Of the toxins, the most highly expressed toxin family was CRiSPs (51%), followed by SVMPIIIs (21.5%). Kunitz-type peptides accounted for 16.6% of the transcriptome (Figure 3).

2.2.4. *Coniophanes schmidtii*

The *C. schmidtii* transcriptome contained 11 toxin families, constituting 38.8% of the TPM within the total DVG transcriptome. SVMPIII was the most highly expressed toxin family (62.7%), followed by NP (12.6%), SVSPs (10.5%), and HYAL (10.4%) (Figure 3).

2.3. Intraspecific Toxin Expression

The samples from the northernmost locality of *C. imperialis* varied somewhat in total toxin expression but expressed the same four toxin families: CRiSP, CTL, 3FTx, and SVMPIII: CRiSPs (34.5%, 39.2%, and 21.5%); CTLs (27.3%, 10.2%, and 27.8%); 3FTx (13.6%, 32.8%, and 25.6%); and SVMPIIIs (12.7%, 15%, and 11.9%) (Figure 4). The southern sample also expressed CRiSP, CTL, and SVMPIII at high levels, but also expressed KUN and Waprin at higher levels than the northern population. Among 60 unique toxin transcripts in the four individuals, 15 were differentially expressed between the northern and southern samples, including five 3FTx and two KUN (Figure 5).

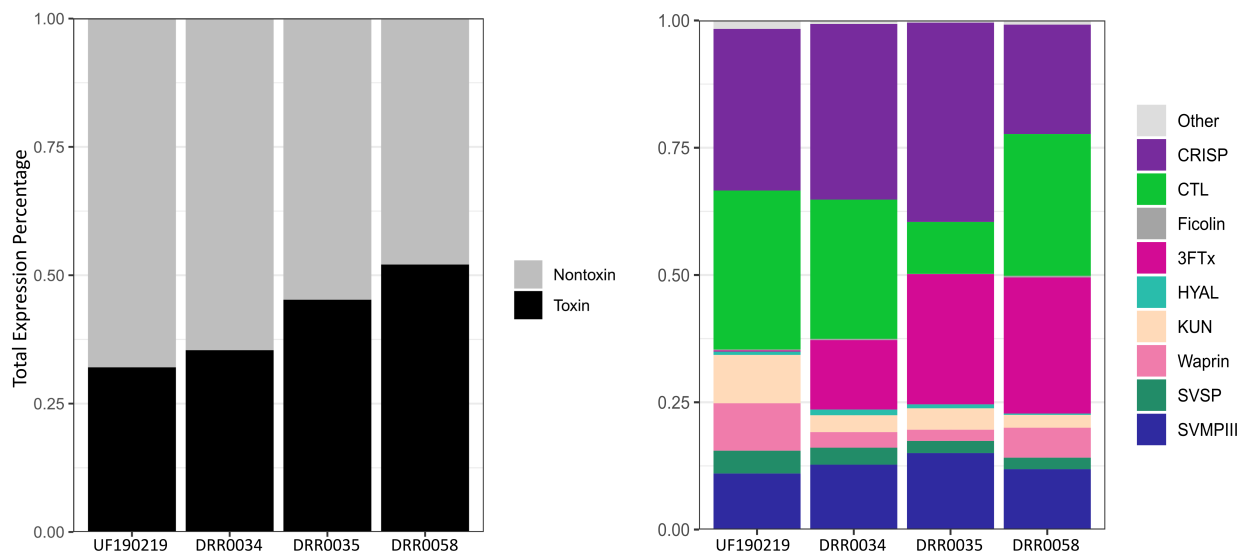


Figure 4. Venom transcriptome characterization for four individuals of *Coniophanes imperialis*. UF190219 denotes the individual from Honduras in contrast with three individuals from south Texas (prefix-DRR). **(Left)** The overall toxin expression percentage for all four individuals. **(Right)** The relative expression of toxin families for all four individuals and proportion of overall toxins each toxin family composes. A figure presenting all toxin families expressed in the transcriptomes can be found in Supplemental Figure S2 (see Supplementary Materials) [CRiSP: cystine-rich secretory proteins, CTL: C-type lectins, 3FTx: three-finger toxins, HYAL: hyaluronidase, KUN: Kunitz-type proteins, SVSP: snake venom serine proteases, SVMPIII: PIII snake venom metalloproteinases].

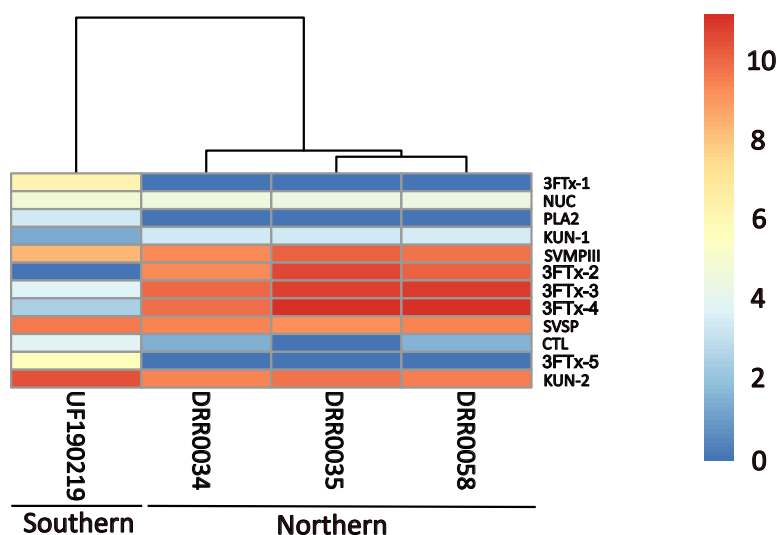


Figure 5. Heat map showing differentially expressed toxins between northern and southern samples of *Coniophanes imperialis*, as determined by DESeq2. Each row represents a specific toxin transcript and expression levels were determined using transcripts-per-million of differentially expressed genes. Rows are organized from least to greatest average expression. [3FTx: three-finger toxins, NUC: Ecto 5' nucleotidase, PLA2: phospholipases A2, KUN: Kunitz-type proteins, SVMPIII: PIII snake venom metalloproteinases, SVSP: snake venom serine proteases, CTL: C-type lectins].

2.4. Venom Proteome

Quantitative mass spectrometry (qMS) on whole venom samples cross-referenced with our Duvernoy's gland transcriptomes allowed us to proteomically confirm the presence of toxins and toxin families in the venom of two individuals of *C. imperialis* (DRR0034 and DRR0035). For DRR0034, we proteomically verified the presence of four toxin families: SVSP, CTL, HYAL, and SVMPIII. For DRR0035, we confirmed the proteomic presence of six toxin families: SVMPIII, CTL, CRiSP, KUN, Waprin, and HYAL. In addition, a putative toxin, Acetylcholinesterase, was also confirmed in the proteome of DRR0035. Multiple SVMPIII proteins were verified within the venom of both DRR0034 and DRR0035, and two CTL proteins were confirmed within the venom of DRR0035.

3. Discussion

In this study, we provide the first published characterization of venom profiles for members of the genus *Coniophanes* and investigated intra- and interspecific variation. By continuing to characterize and assess the venom of overlooked and understudied snake species, we expand our knowledge of venom gene evolution and the scope of phenotypic variation observed in this medically important and fitness-relevant trait. *Coniophanes* appears to possess a potent venom delivery system: our diceCT assessment revealed that *C. fissidens* possesses enlarged teeth attached to the rear of the maxilla. These teeth exhibited clear grooves running down the anterior surface presumably to transfer venom into the bitten organism. Anterior orientation of deep grooves has been proposed to be the greatest degree of specialization for venom delivery found in rear-fanged snakes [44]. Our scans also showed the Duvernoy's gland in close proximity to the enlarged rear fang, highlighting a similar venom apparatus to other medically relevant rear-fanged snakes, such as *Conopsis lineatus* and *Helicops angulatus* (Figure 2) [18,45]. *Coniophanes* also appears to show significant interspecific and intraspecific variation in the presence and expression levels of various toxin families while also potentially retaining fairly conserved venom profiles within localities. In particular, we find that three-finger toxins (3FTx), a prominent

component in the venom of many front-fanged snakes, may be present in some species and localities but devoid in others.

3.1. Toxin Family Expression

All four species of *Coniophanes* investigated in this study exhibited differences in toxin family composition and overall toxin expression levels within the DVG transcriptomes. Most rear-fanged snake venom usually takes the form of either a more neurotoxic venom consisting mostly of 3FTx or a more hemotoxic venom made up of mainly SVMPs and CRiSPs [11]. This trend appears to hold true for *Coniophanes*, with these four species producing either SVMP or CRiSP-dominated venoms. One species (*C. schmidti*) showcased SVMP-dominated venom (with SVMPIIIs composing 62.7% of all toxins), and the three other species displayed CRiSP-dominated venom. However, *C. imperialis* expressed 3FTx at a much higher level than the other species, yet within *C. imperialis*, the individuals from south Texas expressed 3FTx at far higher levels than the individual from the south, with 3FTx, on average, accounting for 24% of all toxins expressed. This variability in venom within the genus, coupled with further variability within specific species, showcases the ability for phenotypic variation that has defined the serpent clade [46].

When assessing venom expression within *C. imperialis*, two primary trends were evident: (1) individuals from Texas had more similar toxin composition to each other than to the individual from Honduras; (2) 3FTx were virtually absent from the expression profile of the Honduran specimen despite making up a sizeable portion of the expression profile in the specimens from Texas, while KUN exhibited much higher expression in the Honduran sample. Notably, both 3FTx and Kunitz-type proteins can act as neurotoxins [47–49]. Perhaps the Kunitz-type proteins in the southern locality play a similar role in prey subjugation to the three-finger toxins in the northern locality. A larger sample size in conjunction with diet studies and biological activity tests will be required to investigate this question further. In addition, the observed variation within *C. imperialis* samples from the extreme northern and southern parts of the range highlights the need for more complete sampling across the entire species distribution.

3.2. Venom Components

3.2.1. SVMPs

P-III subclass snake venom metalloproteinases (SVMPIIIs) were the only toxin family to make up a sizeable portion (>8%) of the Duvernoy's gland transcriptome of every individual (8.1–62.7%); they were also proteomically confirmed in both individuals for which venom samples were collected and analyzed (DRR0034 and DRR0035). These diverse toxins are often associated with the degradation of endothelial cell membranes causing hemorrhagic effects [11,50]. Class III SVMPs are found in a diverse range of snakes, including elapids such as *Ophiophagus hannah*, vipers such as *Daboia russelii*, colubrids such as *Tantilla nigriceps*, and other dipsadids such as *Philodryas olfersii* [22,24,51]. While it is not surprising that SVMPIIIs constitute a key component of *Coniophanes* venom, class III SVMPs were the highest expressed toxin family only in the *C. schmidti* transcriptome. Interestingly, this specimen lacked expression of CRiSPs, which made up almost 40% of the average toxin expression across the other three species sampled and were proteomically confirmed in one individual of *C. imperialis* (DRR0035). The biological effects of CRiSPs are not well characterized; however, research suggests that CRiSPs in snake venom may function either to block Ca²⁺ channels, thus inhibiting smooth muscle contractions, or as cyclic nucleotide-gated (CNG) ion channel blockers [52,53]. Nevertheless, their ecological role in *Coniophanes* venom is difficult to assess [54].

3.2.2. Three-Finger Toxins

We recovered ten unique 3FTx toxins across the four species: seven in *C. imperialis*, two within *C. schmidtii*, and one in *C. lateritius*. Only *C. fissidens* showed no expression of 3FTx transcripts. We found a large reduction in 3FTx in the southern locality of *C. imperialis*. We hypothesize geographic variation in diet within this species may be driving these differences. Three-finger toxins, while consistently found within the venom of rear-fanged snakes, dominate the venom of most elapids [55]. 3FTx attack the nervous system when injected and often take the form of α -Neurotoxins, which induce paralysis by binding to cholinergic receptors thus preventing acetylcholine from binding [56,57]. Importantly, these toxins have been found in and appear to play an important role in the venom of some rear-fanged snakes [7,58]. Previous research has highlighted that in some rear-fanged snakes, 3FTx are closely associated with specific prey. For example, refs. [7,58] found that venom of snakes from the colubroid genus *Boiga* contain 3FTx that are extremely toxic to avian and lizard prey species but have little effect on mammals. In addition, Srodawa et al. [48] found evidence of positive selection on sites within the structural loops of 3FTx in rear-fanged snake venom. These authors posited that these sites may be under selection to better bind to prey-specific molecules. Perhaps 3FTx play a similar role in *Coniophanes* and are highly prey-specific.

3.2.3. Other Venom Components

Other venom components found within the Duvernoy's gland transcriptome of *Coniophanes* included Kunitz-type proteins (KUN), snake venom serine proteinases (SVSPs), and waprins-like proteins. Kunitz-type proteins are the primary component in the venom of black mambas (*Dendroaspis polylepis*), and, as such, are sometimes referred to as "dendrotoxins" [59]. These toxins tend to make up a small portion of most elapid venom (up to 13%) [55]. Kunitz-type proteins normally either prevent protease activity or release acetylcholine to disrupt neuromuscular function and therefore act as neurotoxins [19,47,59]. Kunitz-type proteins were expressed in six of the seven individuals of *Coniophanes*, only absent from the expression profile of *C. schmidtii*. Kunitz-type proteins were proteomically confirmed within the venom of DRR0035.

Snake venom serine proteases tend to be highly expressed in viper venom. These toxins are involved in proteolysis and disrupt coagulation pathways [60]. Despite being most commonly associated with the venom of Viperidae and Crotalidae, SVSPs can be found in Elapidae and rear-fanged snake venom as well. However, within rear-fanged snakes, they have only ever been found in dipsadids [2,18]. SVSPs were also expressed in six of the seven *Coniophanes* individuals, absent only from the expression profile of *C. lateritius*. They tended to compose between 2 and 5% of the total toxins, except in *C. schmidtii*, where they were the third most expressed toxin family and accounted for 10.5% of the total toxins. SVSPs were also proteomically verified in the venom of DRR0034. SVSPs play an important role in many viper venom and are associated with disrupting the haemostatic system through proteolysis and subsequent excessive blood coagulation. These proteins can be found in the venom of Viperidae, Crotalidae, Elapidae, Colubridae, and Dipsadidae [60].

Waprins-like proteins were also found to be expressed in six of the seven *Coniophanes*, and, like SVSPs, *C. lateritius* was the species lacking expression of these transcripts. Waprins tended to be lowly expressed, except for the Honduran individual of *C. imperialis*, for which waprins accounted for 9.3% of the total toxins. Waprins proteins were confirmed within the venom of DRR0035. Waprins have been found in vipers, elapids, colubrids, and dipsadids but are often expressed in very low levels [24,61]. Waprins may function to inhibit proteases, although it is difficult to infer relevance for such lowly expressed proteins [24]. We also

found no evidence of snake venom matrix metalloproteinases (svMMPs) in the venom of *Coniophanes*, supporting previous research suggesting that these toxins are unique to the Xenodontinae subfamily of dipsadids [29].

3.3. Potential Selection by Diet

Despite the limited dietary records, the diet of *Coniophanes* appears diverse and similar across species, although some interspecific and intraspecific variation has been documented. Brown [40] noted that *Coniophanes imperialis* collected from south Texas fed readily on toads. He also observed a toad escape from a *C. imperialis*, only to be dispatched rapidly, presumably from the venom of the bite. In addition, *Coniophanes fissidens*, the only snake in this genus for which we have extensive diet data, does not appear to feed readily on toads. In the single diet study available for *Coniophanes*, Seib [37] examined the stomach contents of 256 specimens of *C. fissidens*, resulting in 127 dietary records, and found only a single example of a toad having been consumed. Interspecific variation in diet is expected considering the extensive range of *Coniophanes* and may explain the observed interspecific venom variation in this genus.

Diet has been closely associated with snake venom in numerous studies, and we posit diet as a putative driver of the observed variation in the venom of *Coniophanes* [1,5,62,63]. We found extensive interspecific venom variation in *Coniophanes*, even in areas of range overlap between species. Specifically, *Coniophanes schmidtii* exhibited a unique venom profile compared to the other species in this study. *C. schmidtii* exhibited much higher expression levels of SVMPs and SVSPs and completely lacked expression of Kunitz-type proteins and CRiSPs. Importantly, the entire distribution of *C. schmidtii* overlaps with the distribution of *C. imperialis*, potentially driving niche partitioning and dietary differences [64]. The subsequent differences in diet may then be responsible for the venom variation between these species, thus producing the unique venom profile of *C. schmidtii*. Intraspecific diet variation has also been documented in *Coniophanes*. Seib [37] recorded diet differences between localities of *C. fissidens*, potentially lending support to the hypothesis that diet variation may be driving venom differences between localities of *C. imperialis*. However, extensive diet research in conjunction with prey toxicity studies will be required to determine the functional implications and environmental drivers of venom variation in this genus.

4. Conclusions

We provide the first venom analysis of four *Coniophanes* species known to inflict medically relevant bites to humans. We find that *Coniophanes* exhibits both interspecific and intraspecific variation in venom components at both presence/absence and expression levels. Certain medically relevant toxin families, such as 3FTx and Kunitz-type proteins, appear highly expressed in some species and completely lacking expression in others. A larger sample size is required to understand the degree of variation across the *Coniophanes* genus. In summary, these findings enrich our understanding of the extent of snake venom variation within small rear-fanged genera. By capturing the variability of venom profiles and further contextualizing them within the venom delivery system, we gain a more integrated view of how these components interact to enable prey capture and defense, even in small, often overlooked taxa. Expanding venom research to species with little or no prior data broadens our understanding of venom evolution over time and provides insights into how different selective pressures shape this ecologically important and medically relevant trait.

5. Materials and Methods

5.1. *Coniophanes* Sampling

We collected *Coniophanes* from three countries (United States, Mexico, and Honduras), representing four species: *C. imperialis*, *C. lateritius*, *C. fissidens*, and *C. schmidtii* (Figure 1). Each species was represented by a single individual except for *C. imperialis*, for which four individuals were collected from two localities: three individuals were collected from south Texas, and a single individual was collected from Cortés, Honduras (Figure 1). All specimens of *Coniophanes* were collected in 2017 or 2018.

5.2. RNA Extraction and Illumina Sequencing

Venom was extracted to stimulate heightened expression levels of toxin genes following the methods from [6]. Four days later, the snakes were sacrificed [65] and Duvernoy's glands were dissected and stored in RNAlater at -80°C . We used a standard TRIzol RNA extraction to obtain RNA from the left and right DVG separately following the methods of [61]. We first diced up the DVGs and placed them into a TRIzol solution. Then, the mixture was homogenized and relocated into a phase lock heavy gel tube. After cell lysis, we used chloroform to separate the total RNA, and the RNA was purified using isopropyl alcohol and ethanol precipitation. A Qubit RNA BroadRange Assay (Thermo Fisher Scientific, Waltham, MA, USA) was used to assess the concentration of total RNA to ensure sufficient RNA quantity for library preparations. RNA quality was assessed using an Agilent Bioanalyzer 2100 and an RNA 6000 Pico Kit (Agilent Technologies, Santa Clara, CA, USA).

Next, we created cDNA libraries using magnetic beads to isolate mRNA, and then the cDNA was synthesized and amplified with PCR following the methods of [66]. In brief, we used a NEBNext Poly(A) mRNA Magnetic Isolation Module with equivalent mRNA from both the left and right DVGs. After magnetic bead isolation, we followed the manufacturer's protocols to prepare cDNA libraries using a NEBNext Ultra RNA Library Prep Kit for Illumina (San Diego, CA, USA). A fragmentation time of 13.5 min produced a mean fragment size of 400 bp and 14 cycles of PCR amplification of the cDNA libraries. Next, we evaluated the quality and yield of the libraries with a Bioanalyzer 2100 using a DNA High Sensitivity Kit (Agilent Technologies). KAPA qPCR was then used to individually determine the overall amplifiable concentration of the cDNA libraries. All samples were then pooled and assessed with the Bioanalyzer. Finally, the libraries were paired-end sequenced at 150 bp using Illumina sequencing technologies within the College of Medicine Translational Science Laboratory at Florida State University (Tallahassee, FL, USA).

5.3. Transcriptome Annotation

The Duvernoy's gland transcriptomes were assembled and annotated following the manual annotation methods outlined in [18] combined with the ToxCodan pipeline from [6]. In brief, left and right DVG sequenced reads were merged and then trimmed using Trim Galore! v.0.6.7 (<https://github.com/FelixKrueger/TrimGalore>, accessed on 19 June 2023). Forward and backward reads were paired using Paired-End Read Merger (PEAR v.0.9.11) [67]. Next, Extender v.0 [66] and Trinity v.2.14.0 [68] were used to assemble reads into contigs. Assemblies were combined, and then identical contigs were removed with cd-hit-est [69]. Following this, ToxCodan v.0 [70] pipeline was used to annotate toxins. Then, we searched for toxins in BLAST v.2.14.0, referencing the SwissProt database and custom Python v.3.7.12 scripts to filter results. The Codan pipeline was applied after ToxCodan to the nontoxins to predict coding sequence regions using the vertebrate models. Geneious Prime 2024.0 (<https://geneious.com>) was used to manually inspect open reading frames (ORFs) to identify toxins missed by our custom Python scripts. The annotation from ToxCodan and

custom scripts were merged, and duplicated sequences were removed. Next, a custom script (<https://github.com/masonaj157/ChimeraKiller>, accessed on 30 September 2023) was used to remove “chimeras” (the accidental merging of two or more transcripts). Then, we reduced allelic variation using *cd-hit-est* at 98% [69] and mapped the reads back to the transcriptome using *BWA-MEM* v.0.7.17-r1188 [71]. Any transcripts with less than 5× coverage for more than 10% of the transcriptome were removed [72]. We also used a custom script to remove sequences with internal stop codons or those lacking stop codons. Then, we used RNA-seq by Expectation Maximization (RSEM) to estimate expression levels of each transcript [61,66,73]. Results from RSEM were plotted in R v.4.3.2 (R Core Team 2023).

5.4. Differential Expression

To investigate potential intraspecific variation of venom production among *C. imperialis* individuals, we used a differential gene expression analysis to examine differences in venom gene expression in *Coniophanes imperialis* between the three individuals from the northern locality and the individual from the southern locality. We accomplished this using the DESeq2 package in R with a false discovery rate threshold of >0.05 [74].

5.5. Proteomics

We performed reversed-phase high-performance liquid chromatography (RP-HPLC) on venom samples from two individuals of *C. imperialis*: DRR0034 and DRR0035. The RP-HPLC was performed using a Prominence HPLC System (Shimadzu Scientific Instruments, Kyoto, Japan). Centrifugation was used to remove insoluble material after the dry venom samples were suspended in water. A Nanodrop 2000c Spectrophotometer (Thermo Fisher Scientific) was then used to assess the concentration of venom. We then added 15 µg of venom to an Aeris 3.6 µm WIDEPORÉ XB-C18 (250 mm length; 2.1 mm internal diameter) column (Phenomenex, Torrance, CA, USA). The aeris utilized a detection wavelength of 220 nm and a SIL-30 AC autosampler (Shimadzu Scientific Instruments, Kyoto, Japan). The standard solvent system was A = 0.1% trifluoroacetic acid (TFA) in water and B = 0.06% TFA in acetonitrile. We ran both samples with a 0.2 mL/min flow rate for a 125 min gradient. The gradient began at 10% B for five min, then increased to 55% B for 110 min, then increased again to 75% for five min and remained at 75% B for five more minutes before being washed for 15 min with 10% B.

We used quantitative mass spectrometry (qMS) on two *Coniophanes imperialis* venom samples to proteomically verify toxin expression following [61]. We quantified protein samples using the Qubit Protein Assay kit with a Qubit 1.0 Fluorometer (Thermo Fisher Scientific). This was accomplished first by adding 11 µg of each venom sample to 150 µg of 100 mM Ammonium Bicarbonate for 20 min. Next, using the Calbiochem ProteoExtract All-in-One Trypsin Digestion Kit (Merck, Darmstadt, Germany) according to the manufacturer’s instructions and using LC/MS grade solvents, 30 µL of 10 mM Dithiothreitol was added to the solutions and incubated for 1 h at 60 °C. Following incubation, 30 µL of 50 mM Iodoacetoamine was added as well. Thirty minutes later, 150 µL of 50 mM Ammonium Bicarbonate was added to the solutions. We then added Trypsin at 0.5 µg/2.5 µL diluted in 50 mM Ammonium Bicarbonate for digestion and incubated the mixture for 18 h at 37 °C. Lastly, to stop digestion, 1% Trifluoroacetic acid at 5% volume of the solution was added. We then dried both samples using a SpeedVac at 25 °C for 1 h and stored them at −20 °C until use for qMS. We redissolved the resulting dried and digested tryptic peptides in 0.1% formic acid to produce a final concentration of 250 ng/µL for mass spectrometry. We used three digested *Escherichia coli* proteins as internal standards. They were purchased from Abcam (Waltham, MA, USA) at known concentrations, and we mixed the bacteria at the following proportions (1000×) before digestion: 25 fmol of P00811 (Beta-lactamase ampC),

250 fmol of P31658 (Protein deglycase 1), and 2500 fmol of P31697 (Chaperone protein FimC) per injection. To yield the desired final concentration, we took the internal standard peptide mix and infused them into the sample.

After this, we prepared for the LC-MS/MS run by analyzing a 2 μ L aliquot of each sample using an externally calibrated Thermo Q Exactive HF (high-resolution electrospray tandem mass spectrometer) along with the Dionex UltiMate 3000 RSLCnano System (Dionex Corporation, Sunnyvale, CA, USA). Then, the samples were aspirated into a 50 μ L loop and subsequently loaded onto the trap column (Thermo μ -Precolumn 5 mm, with nanoViper tubing 30 μ m i. d. \times 10 cm). In order to achieve separation via the analytical column (Acclaim Pepmap RSLC (Thermo Fisher Scientific, Waltham, MA, USA) 75 μ M \times 15 cm nanoviper), we set the flow rate to 300 nl/min. The phases were composed as follows: mobile phase A = 99.9% H₂O (EMD Omni Solvent) plus 0.1% formic acid; mobile phase B = 99.9% ACN plus 0.1% formic acid. We then conducted a 60 min linear gradient from 3% to 45% B. Then, we nanosprayed the LC eluent into the Q Exactive HF mass spectrometer (Thermo Scientific). The Q Exactive HF was incorporated into a data-dependent mode under the control of the Thermo Excalibur 3.1.66 (Thermo Scientific). We then downloaded the MS data using a data-dependent method for the Q Exactive HF platform. This platform uses survey scans to identify the precursor ions that are highest in abundance and have not been sequenced yet. Then, the samples were sequenced using higher energy collisional dissociation fragmentation using predictive automatic gain control to produce a target value of 105 ions. We conducted our scans (350–1700 m/z) in profile mode with a resolution of 60,000. To acquire the MS₂, we used centroid mode and a resolution of 15,000. All ions with a single charge, a charge greater than seven, or those with unassigned ions were excluded. We also used a 15 s dynamic exclusion window and conducted measurements at room temperature. To account for potential machine variability and to produce label-free quantification, we used three technical replicates.

Proteome Discoverer v.2.2 (Thermo Fisher Scientific) facilitated our search of the raw files using the SequestHT search engine along with custom-generated FASTA databases built from the de novo-assembled transcripts for *C. imperialis*. The SequestHT search parameters were as follows: enzyme name = Trypsin, minimum peptide length = 6, maximum peptide length = 144, maximum missed cleavage = 2, maximum delta Cn = 0.05, precursor mass tolerance = 10 ppm, carbamidomethyl + 57.021 Da(C), fragment mass tolerance = 0.2 Da, dynamic modifications, and oxidation + 15.995 Da(M). We performed all searches twice. We first used embloss with the following specs: getorf-find 1-minsize 90 on all open-reading frames (ORFs) in the transcriptome assembly to check for toxins that could be missing from our transcriptomes. We conducted the second search against our final completed transcriptome. This included all curated toxin sequences so that we could proteomically confirm toxin presence in our venom samples. The identity of the proteins were validated with Scaffold v.4.10.0 (Proteome Software Inc., Portland, OR, USA). We used 1.0% false discovery rate (FDR) to identify proteins using the Scaffold Local FDR algorithm with a minimum of one recognized peptide. All transcripts were considered proteomically confirmed if we detected it in any of the three replicates across either sample. We treated proteins individually if they were grouped by Scaffold because of shared peptide evidence instead of treating them as a cluster in order to assign the peptide directly to the corresponding transcript.

5.6. DiceCT

To visualize the venom delivery system of *Coniophanes*, we used diffusible iodine-based contrast-enhanced computed tomography (diceCT) to visualize the Duvernoy's gland and enlarged rear fang of *Coniophanes fissidens* [45]. A preserved adult museum specimen of

C. fissidens (UMMZ Herps 87643) from the University of Michigan Museum of Zoology collected from Chiapas, Mexico, in 1937 was stained for seven days in a 1.25% Lugol's iodine solution. The specimen was then scanned using the University of Michigan's Nikon XT H 225 ST μ CT scanner (Nikon Corporation, Tokyo, Japan). The *C. fissidens* voxel size was 17 microns, using 100 kilovolts, 200 micro-amperes, a 250-millisecond exposure, and 3141 projections with 16 \times frames on average. Three-dimensional renderings of the specimen were produced using Volume Graphics Studio Max (v.2024.1 Heidleberg, Germany) software. The Duvernoy's gland and enlarged rear fangs were segmented to show location within the skull and proximity to each other.

Supplementary Materials: The following supporting information can be downloaded at <https://www.mdpi.com/article/10.3390/toxins18020108/s1>, Figure S1: Venom transcriptome characterization for four species of *Coniophanes* showing all toxin families expressed; Figure S2: Venom transcriptome characterization for four individuals of *Coniophanes imperialis* showing all toxin families expressed.

Author Contributions: Conceptualization: J.H.F. and C.L.P.; investigation, methodology, and formal analyses: J.H.F., R.A.R.-G., R.M.R., A.J.M., M.P.H., E.P.H., R.N., M.B., L.H. and G.C.-G.; writing—original draft: J.H.F.; writing—review and editing: all authors; data curation: J.H.F., R.A.R.-G., R.N. and C.L.P.; resources and funding acquisition: C.L.P., D.R.R. and A.R.D.R. All authors have read and agreed to the published version of the manuscript.

Funding: This research was funded by the National Science Foundation (DEB 1638879 & 1822417 to C.L.P., DEB 2141892 to A.R.D.R., DBI 20409901 to MPH and DEB 1638902 to D.R.R.). This research was made possible, in part, with support from the Clemson University Genomics and Bioinformatics Facility, which receives support from the College of Science, and two Institutional Development Awards (IDeA) from the National Institute of General Medical Sciences of the National Institutes of Health under grant numbers P20GM146584 and P20GM139769.

Institutional Review Board Statement: Animal work was approved by the Clemson University Institute for Animal Care and Use Committee #2017-067 and Florida State University IACUC protocols 0924, 1230, 1333, 1529, and 1836. Honduras: ICF: RESOLUCIÓN-DE-MP-067-2018.

Data Availability Statement: Specimen citation: "ummz-herps-87643 *Coniophanes fissidens*" in the digital collection University of Michigan Museum of Zoology, Reptiles and Amphibians Catalogue: <https://quod.lib.umich.edu/a/amph3ic/x-87643/nofile> (University of Michigan Library Digital Collections, accessed on 5 September 2024). GBIF Occurrence data accessed via GBIF.org (2 September 2025) GBIF Occurrence Download: <https://doi.org/10.15468/dl.jx9hjg> (*C. lateritius*). GBIF.org (4 September 2025) GBIF Occurrence Download: <https://doi.org/10.15468/dl.y67svd> (*C. imperialis*). GBIF.org (5 September 2025) GBIF Occurrence Download: <https://doi.org/10.15468/dl.uydgfp> (*C. schmidt*). GBIF.org (5 September 2025) GBIF Occurrence Download: <https://doi.org/10.15468/dl.bsvc4n> (*C. fissidens*). The raw sequence data for the Duvernoy's gland transcriptomes are available on NCBI SRA under BioProject PRJNA88989 (SAMN53244439–SAMN53244433). SRR accession numbers SRR36021064–SRR36021070.

Acknowledgments: We would like to thank Diego Quirola, Matthew McTernan, Taryn Cornell and former Parkinson Lab members for comments and discussions regarding all aspects of this project. We thank Josiah "Joe" Townsend, Emmanuel Orellana, and Carlos Andino for help in planning, participating, and facilitating the collection of the Honduras individuals, and Sam Manatt for allowing access to his property for collecting specimens. We would also like to thank Javier A. Ortiz-Medina, Bianca Sabido-Alpuche, Marcos Meneses-Millán, Jason Jones, Ricardo Ramirez, Chris Grünwald, and Hector Franz for help in facilitating field work in Mexico.

Conflicts of Interest: The authors declare no conflicts of interest. The funders had no role in the design of the study; in the collection, analyses, or interpretation of data; in the writing of the manuscript; or in the decision to publish the results.

References

1. Mason, A.J.; Holding, M.L.; Rautsaw, R.M.; Rokyta, D.R.; Parkinson, C.L.; Gibbs, H.L. Venom Gene Sequence Diversity and Expression Jointly Shape Diet Adaptation in Pitvipers. *Mol. Biol. Evol.* **2022**, *39*, msac082. [[CrossRef](#)]
2. Junqueira-de Azevedo, I.; Campos, P.; Ching, A.; Mackessy, S. Colubrid Venom Composition: An -Omics Perspective. *Toxins* **2016**, *8*, 230. [[CrossRef](#)]
3. Ferreira-Rodrigues, S.C.; Silva, R.C.C.; Trevisan, M.; Rodrigues, P.S.M.; Del-Rei, T.H.M.; Sousa, L.F.; Vilarinho, A.R.G.; Lima, C.A.; Rodrigues, J.L.; Silva, M.M.R.; et al. Ontogenetic and sexual differences in the venom of *Bothrops moojeni*: Insights from a litter and its mother. *Braz. J. Biol.* **2024**, *84*, e279474. [[CrossRef](#)]
4. van Thiel, J.; Alonso, L.L.; Slagboom, J.; Dunstan, N.; Wouters, R.M.; Modahl, C.M.; Vonk, F.J.; Jackson, T.N.W.; Kool, J. Highly Evolvable: Investigating Interspecific and Intraspecific Venom Variation in Taipans (*Oxyuranus* spp.) and Brown Snakes (*Pseudonaja* spp.). *Toxins* **2023**, *15*, 74. [[CrossRef](#)]
5. Holding, M.L.; Strickland, J.L.; Rautsaw, R.M.; Hofmann, E.P.; Mason, A.J.; Hogan, M.P.; Nystrom, G.S.; Ellsworth, S.A.; Colston, T.J.; Borja, M.; et al. Phylogenetically diverse diets favor more complex venoms in North American pitvipers. *Proc. Natl. Acad. Sci. USA* **2021**, *118*, e2015579118. [[CrossRef](#)]
6. Heptinstall, T.C.; Strickland, J.L.; Rosales-Garcia, R.A.; Rautsaw, R.M.; Simpson, C.L.; Nystrom, G.S.; Ellsworth, S.A.; Hogan, M.P.; Borja, M.; Fernandes Campos, P.; et al. Venom phenotype conservation suggests integrated specialization in a lizard-eating snake. *Toxicon* **2023**, *229*, 107135. [[CrossRef](#)] [[PubMed](#)]
7. Pawlak, J.; Mackessy, S.P.; Fry, B.G.; Bhatia, M.; Mourier, G.; Fruchart-Gaillard, C.; Servent, D.; Ménez, R.; Stura, E.; Ménez, A.; et al. Denmotoxin, a Three-finger Toxin from the Colubrid Snake *Boiga dendrophila* (Mangrove Catsnake) with Bird-specific Activity. *J. Biol. Chem.* **2006**, *281*, 29030–29041. [[CrossRef](#)] [[PubMed](#)]
8. Bucciarelli, G.M.; Alsalek, F.; Kats, L.B.; Green, D.B.; Shaffer, H.B. Toxic Relationships and Arms-Race Coevolution Revisited. *Annu. Rev. Anim. Biosci.* **2022**, *10*, 63–80. [[CrossRef](#)]
9. Calvete, J.J.; Sanz, L.; Angulo, Y.; Lomonte, B.; Gutiérrez, J.M. Venoms, venomics, antivenomics. *FEBS Lett.* **2009**, *583*, 1736–1743. [[CrossRef](#)] [[PubMed](#)]
10. Dowell, N.; Giorgianni, M.; Kassner, V.; Selegue, J.; Sanchez, E.; Carroll, S. The Deep Origin and Recent Loss of Venom Toxin Genes in Rattlesnakes. *Curr. Biol.* **2016**, *26*, 2434–2445. [[CrossRef](#)]
11. Modahl, C.M.; Mackessy, S.P. Venoms of Rear-Fanged Snakes: New Proteins and Novel Activities. *Front. Ecol. Evol.* **2019**, *7*, 279. [[CrossRef](#)]
12. Hargreaves, A.D.; Swain, M.T.; Hegarty, M.J.; Logan, D.W.; Mulley, J.F. Restriction and Recruitment—Gene Duplication and the Origin and Evolution of Snake Venom Toxins. *Genome Biol. Evol.* **2014**, *6*, 2088–2095. [[CrossRef](#)]
13. Modahl, C.M.; Saviola, A.J.; Mackessy, S.P. Venoms of Colubrids. In *Venom Genomics and Proteomics*; Gopalakrishnakone, P., Calvete, J.J., Eds.; Springer: Dordrecht, The Netherlands, 2016; pp. 51–79. [[CrossRef](#)]
14. Savitzky, A.H. The Role of Venom Delivery Strategies in Snake Evolution. *Evolution* **1980**, *34*, 1194–1204. [[CrossRef](#)]
15. Vonk, F.J.; Admiraal, J.F.; Jackson, K.; Reshef, R.; de Bakker, M.A.G.; Vanderschoot, K.; van den Berge, I.; van Atten, M.; Burgerhout, E.; Beck, A.; et al. Evolutionary origin and development of snake fangs. *Nature* **2008**, *454*, 630–633. [[CrossRef](#)]
16. Mackessy, S.P.; Saviola, A.J. Understanding Biological Roles of Venoms Among the Caenophidia: The Importance of Rear-Fanged Snakes. *Integr. Comp. Biol.* **2016**, *56*, 1004–1021. [[CrossRef](#)]
17. Weinstein, S.A.; Warrell, D.A.; Keyler, D.E. Chapter 2—Differences between buccal gland secretion and associated venom delivery systems of front-fanged snakes and non-front-fanged snakes: Low- versus high-pressure gland function and canaliculated versus solid dentition. In *“Venomous” Bites from “Non-Venomous” Snakes*, 2nd ed.; Elsevier: Boston, MA, USA, 2022; Chapter 2, pp. 41–80. [[CrossRef](#)]
18. Schramer, T.D.; Rautsaw, R.M.; Bayona-Serrano, J.D.; Nystrom, G.S.; West, T.R.; Ortiz-Medina, J.A.; Sabido-Alpuche, B.; Meneses-Millán, M.; Borja, M.; Junqueira-de Azevedo, I.L.M.; et al. An integrative view of the toxic potential of *Conopsis lineatus* (Dipsadidae: Xenodontinae), a medically relevant rear-fanged snake. *Toxicon* **2022**, *205*, 38–52. [[CrossRef](#)]
19. Entiauspe-Neto, O.M.; Nachtigall, P.G.; Borges-Martins, M.; Junqueira-de Azevedo, I.L.M.; Grazziotin, F.G. Highly conserved and extremely variable: The paradoxical pattern of toxin expression revealed by comparative venom-gland transcriptomics of *Phalotris* (Serpentes: Dipsadidae). *Toxicon* **2024**, *244*, 107740. [[CrossRef](#)] [[PubMed](#)]
20. Gutiérrez, J.M.; Calvete, J.J.; Habib, A.G.; Harrison, R.A.; Williams, D.J.; Warrell, D.A. Snakebite envenoming. *Nat. Rev. Dis. Prim.* **2017**, *3*, 17063. [[CrossRef](#)]
21. Perry, G.; Lacy, M.; Das, I. Snakes, Snakebites, and Humans. In *Problematic Wildlife II: New Conservation and Management Challenges in the Human-Wildlife Interactions*; Angelici, F.M., Rossi, L., Eds.; Springer International Publishing: Cham, Switzerland, 2020; pp. 561–580. [[CrossRef](#)]
22. Hofmann, E.P.; Rautsaw, R.M.; Mason, A.J.; Strickland, J.L.; Parkinson, C.L. Duvernoy’s Gland Transcriptomics of the Plains Black-Headed Snake, *Tantilla nigriceps* (Squamata, Colubridae): Unearthing the Venom of Small Rear-Fanged Snakes. *Toxins* **2021**, *13*, 336. [[CrossRef](#)] [[PubMed](#)]

23. Serrano, F.C.; Pontes-Nogueira, M.; Sawaya, R.J.; Alencar, L.R.V.; Nogueira, C.C.; Grazziotin, F.G. There and back again: When and how the world's richest snake family (Dipsadidae) dispersed and speciated across the Neotropical region. *J. Biogeogr.* **2024**, *51*, 878–893. [[CrossRef](#)]
24. Tioyama, E.C.; Bayona-Serrano, J.D.; Portes-Junior, J.A.; Nachtigall, P.G.; de Souza, V.C.; Beraldo-Neto, E.; Grazziotin, F.G.; Junqueira-de Azevedo, I.L.M.; Moura-da Silva, A.M.; Freitas-de Sousa, L.A. The Venom Composition of the Snake Tribe Philodryadini: 'Omic' Techniques Reveal Intergeneric Variability among South American Racers. *Toxins* **2023**, *15*, 415. [[CrossRef](#)]
25. Mackessy, S.P. Biochemistry and Pharmacology of Colubrid Snake Venoms. *J. Toxicol. Toxin Rev.* **2002**, *21*, 43–83. [[CrossRef](#)]
26. Ching, A.T.C.; Paes Leme, A.F.; Zelanis, A.; Rocha, M.M.T.; Furtado, M.d.F.D.; Silva, D.A.; Trugilho, M.R.O.; da Rocha, S.L.G.; Perales, J.; Ho, P.L.; et al. Venomics Profiling of *Thamnodynastes strigatus* Unveils Matrix Metalloproteinases and Other Novel Proteins Recruited to the Toxin Arsenal of Rear-Fanged Snakes. *J. Proteome Res.* **2012**, *11*, 1152–1162. [[CrossRef](#)] [[PubMed](#)]
27. Komori, K.; Konishi, M.; Maruta, Y.; Toriba, M.; Sakai, A.; Matsuda, A.; Hori, T.; Nakatani, M.; Minamino, N.; Akizawa, T. Characterization of a Novel Metalloproteinase in Duvernoy's Gland of *Rhabdophis tigrinus tigrinus*. *J. Toxicol. Sci.* **2006**, *31*, 157–168. [[CrossRef](#)] [[PubMed](#)]
28. Campos, P.F.; Andrade-Silva, D.; Zelanis, A.; Paes Leme, A.F.; Rocha, M.M.T.; Menezes, M.C.; Serrano, S.M.; Junqueira-de Azevedo, I.d.L.M. Trends in the Evolution of Snake Toxins Underscored by an Integrative Omics Approach to Profile the Venom of the Colubrid *Phalotris mertensi*. *Genome Biol. Evol.* **2016**, *8*, 2266–2287. [[CrossRef](#)] [[PubMed](#)]
29. Bayona-Serrano, J.D.; Viala, V.L.; Rautsaw, R.M.; Schramer, T.D.; Barros-Carvalho, G.A.; Nishiyama, M.Y., Jr.; Freitas-de Sousa, L.A.; Moura-da Silva, A.M.; Parkinson, C.L.; Grazziotin, F.G.; et al. Replacement and Parallel Simplification of Nonhomologous Proteinases Maintain Venom Phenotypes in Rear-Fanged Snakes. *Mol. Biol. Evol.* **2020**, *37*, 3563–3575. [[CrossRef](#)]
30. Saviola, A.J.; Peichoto, M.E.; Mackessy, S.P. Rear-fanged snake venoms: An untapped source of novel compounds and potential drug leads. *Toxin Rev.* **2014**, *33*, 185–201. [[CrossRef](#)]
31. Angarita-Sierra, T.; Montañez-Méndez, A.; Toro-Sánchez, T.; Rodríguez-Vargas, A. A case of envenomation by the false fer-de-lance snake *Leptodeira annulata* (Linnaeus, 1758) in the department of La Guajira, Colombia. *Biomédica* **2020**, *40*, 20–26. [[CrossRef](#)]
32. da Graca Salomao, M.; Albolea, A.B.P.; Almeida Santos, S.M. Colubrid Snakebite: A Public Health Problem in Brazil. *Herpetol. Rev.* **2003**, *34*, 307–312.
33. Cadle, J.E. A New Species of *Coniophanes* (Serpentes: Colubridae) from Northwestern Peru. *Herpetologica* **1989**, *45*, 411–424.
34. Hernández-González, J.; Vásquez-Cruz, V. *Coniophanes fissidens*. *Herpetol. Rev.* **2024**, *55*, 275–276.
35. Cedeño-Vázquez, J.R.; Huerta Hernández, E.J.; Beutelspacher-García, P.M. *Coniophanes imperialis* (Regal Black-striped Snake). Diet, foraging, and predation behavior. *Herpetol. Rev.* **2024**, *55*, 276–277.
36. Carbajal Márquez, R.A.; García Balderas, C.M.; Ramírez Valverde, T.; Cedeño Vázquez, J.R.; Blanco Campos, N.G. New prey items in the diet of snakes from the Yucatán Peninsula, Mexico. *Cuad. Herpetol.* **2019**, *33*, 71–74. [[CrossRef](#)]
37. Seib, R.L. Euryphagy in a Tropical Snake, *Coniophanes fissidens*. *Biotropica* **1985**, *17*, 57–64. [[CrossRef](#)]
38. Saporito, R.A.; Zuercher, R.; Roberts, M.; Gerow, K.G.; Donnelly, M.A. Experimental Evidence for Aposematism in the Dendrobatid Poison Frog *Oophaga pumilio*. *Copeia* **2007**, *2007*, 1006–1011. [[CrossRef](#)]
39. Köhler, G.; Cedeño-Vázquez, J.R.; Akary, M.T.; Beutelspacher-García, P.M. The Chetumal Snake Census: Generating biological data from road-killed snakes. Part 4. *Coniophanes imperialis*, *C. meridanus*, and *C. schmidti*. *Mesoamerican Herpetol.* **2017**, *4*, 528–542.
40. Brown, B.C. Notes on *Coniophanes imperialis* (Baird). *Copeia* **1937**, *1937*, 234–234. [[CrossRef](#)]
41. Brown, B.C. The Effect of *Coniophanes* Poisoning in Man. *Copeia* **1939**, *1939*, 109–109. [[CrossRef](#)]
42. McKinstry, D.M. Evidence of toxic saliva in some colubrid snakes of the United States. *Toxicon* **1978**, *16*, 523–534. [[CrossRef](#)]
43. Gutiérrez, J.M.; Sasa, M. Bites and Envenomations by Colubrid Snakes in Mexico and Central America. *J. Toxicol. Toxin Rev.* **2002**, *21*, 105–115. [[CrossRef](#)]
44. Jackson, K.; Fritts, T.H. Evidence from tooth surface morphology for a posterior maxillary origin of the proteroglyph fang. *Amphibia-Reptilia* **1995**, *6*, 273–288. [[CrossRef](#)]
45. Callahan, S.; Crowe-Riddell, J.M.; Nagesan, R.S.; Gray, J.A.; Davis Rabosky, A.R. A guide for optimal iodine staining and high-throughput diceCT scanning in snakes. *Ecol. Evol.* **2021**, *11*, 11587–11603. [[CrossRef](#)]
46. Title, P.O.; Singhal, S.; Grundler, M.C.; Costa, G.C.; Pyron, R.A.; Colston, T.J.; Grundler, M.R.; Prates, I.; Stepanova, N.; Jones, M.E.H.; et al. The macroevolutionary singularity of snakes. *Science* **2024**, *383*, 918–923. [[CrossRef](#)] [[PubMed](#)]
47. Saldarriaga-Córdoba, M.; Clavero-León, C.; Rey-Suarez, P.; Nuñez-Rangel, V.; Avendaño-Herrera, R.; Solano-González, S.; Alzate, J.F. Unveiling Novel Kunitz- and Waprin-Type Toxins in the *Micrurus mipartitus* Coral Snake Venom Gland: An In Silico Transcriptome Analysis. *Toxins* **2024**, *16*, 224. [[CrossRef](#)] [[PubMed](#)]
48. Srodawa, K.; Cerda, P.A.; Davis Rabosky, A.R.; Crowe-Riddell, J.M. Evolution of Three-Finger Toxin Genes in Neotropical Colubrine Snakes (Colubridae). *Toxins* **2023**, *15*, 523. [[CrossRef](#)]

49. Fry, B.G.; Wüster, W. Assembling an Arsenal: Origin and Evolution of the Snake Venom Proteome Inferred from Phylogenetic Analysis of Toxin Sequences. *Mol. Biol. Evol.* **2004**, *21*, 870–883. [[CrossRef](#)]
50. Slagboom, J.; Kool, J.; Harrison, R.A.; Casewell, N.R. Haemotoxic snake venoms: Their functional activity, impact on snakebite victims and pharmaceutical promise. *Br. J. Haematol.* **2017**, *177*, 947–959. [[CrossRef](#)]
51. Olaoba, O.T.; Karina dos Santos, P.; Selistre-de Araujo, H.S.; Ferreira de Souza, D.H. Snake Venom Metalloproteinases (SVMPs): A structure-function update. *Toxicon X* **2020**, *7*, 100052. [[CrossRef](#)] [[PubMed](#)]
52. Yamazaki, Y.; Koike, H.; Sugiyama, Y.; Motoyoshi, K.; Wada, T.; Hishinuma, S.; Mita, M.; Morita, T. Cloning and characterization of novel snake venom proteins that block smooth muscle contraction. *Eur. J. Biochem.* **2002**, *269*, 2708–2715. [[CrossRef](#)]
53. Yamazaki, Y.; Morita, T. Structure and function of snake venom cysteine-rich secretory proteins. *Toxicon* **2004**, *44*, 227–231. [[CrossRef](#)]
54. Tadokoro, T.; M. Modahl, C.; Maenaka, K.; Aoki-Shioi, N. Cysteine-Rich Secretory Proteins (CRISPs) from Venomous Snakes: An Overview of the Functional Diversity in a Large and Underappreciated Superfamily. *Toxins* **2020**, *12*, 175. [[CrossRef](#)]
55. Tasoulis, T.; Isbister, G.K. A Review and Database of Snake Venom Proteomes. *Toxins* **2017**, *9*, 290. [[CrossRef](#)]
56. Fry, B.G.; Lumsden, N.G.; Wüster, W.; Wickramaratna, J.C.; Hodgson, W.C.; Manjunatha Kini, R. Isolation of a Neurotoxin (α -colubritoxin) from a Nonvenomous Colubrid: Evidence for Early Origin of Venom in Snakes. *J. Mol. Evol.* **2003**, *57*, 446–452. [[CrossRef](#)]
57. Tsetlin, V.I. Three-finger snake neurotoxins and Ly6 proteins targeting nicotinic acetylcholine receptors: Pharmacological tools and endogenous modulators. *Trends Pharmacol. Sci.* **2015**, *36*, 109–123. [[CrossRef](#)]
58. Pawlak, J.; Kini, R.M. Unique gene organization of colubrid three-finger toxins: Complete cDNA and gene sequences of denmotoxin, a bird-specific toxin from colubrid snake *Boiga dendrophila* (Mangrove Catsnake). *Biochimie* **2008**, *90*, 868–877. [[CrossRef](#)]
59. Drogenik, S.; Leonardi, A.; Žužek, M.C.; Frangež, R.; Križaj, I. The first Kunitz-type proteins from a viperid venom that potentiate neuromuscular transmission. *Toxicon* **2020**, *187*, 262–270. [[CrossRef](#)]
60. Serrano, S.M.T.; Maroun, R.C. Snake venom serine proteinases: Sequence homology vs. substrate specificity, a paradox to be solved. *Toxicon* **2005**, *45*, 1115–1132. [[CrossRef](#)]
61. Hofmann, E.P.; Rautsaw, R.M.; Strickland, J.L.; Holding, M.L.; Hogan, M.P.; Mason, A.J.; Rokyta, D.R.; Parkinson, C.L. Comparative venom-gland transcriptomics and venom proteomics of four Sidewinder Rattlesnake (*Crotalus cerastes*) lineages reveal little differential expression despite individual variation. *Sci. Rep.* **2018**, *8*, 15534. [[CrossRef](#)] [[PubMed](#)]
62. Lyons, K.; Dugon, M.M.; Healy, K. Diet Breadth Mediates the Prey Specificity of Venom Potency in Snakes. *Toxins* **2020**, *12*, 74. [[CrossRef](#)] [[PubMed](#)]
63. Davies, E.L.; Arbuckle, K. Coevolution of Snake Venom Toxic Activities and Diet: Evidence that Ecological Generalism Favours Toxicological Diversity. *Toxins* **2019**, *11*, 711. [[CrossRef](#)] [[PubMed](#)]
64. Luiselli, L.; Rugiero, L. Food Niche Partitioning by Water Snakes (Genus *Natrix*) at a Freshwater Environment in Central Italy. *J. Freshw. Ecol.* **1991**, *6*, 439–444. [[CrossRef](#)]
65. Rotenberg, D.; Bamberger, E.S.; Kochva, E. Studies on ribonucleic acid synthesis in the venom glands of *Vipera palaestinae* (Ophidia, Reptilia). *Biochem. J.* **1971**, *121*, 609–612. [[CrossRef](#)] [[PubMed](#)]
66. Rokyta, D.R.; Lemmon, A.R.; Margres, M.J.; Aronow, K. The venom-gland transcriptome of the eastern diamondback rattlesnake (*Crotalus adamanteus*). *BMC Genom.* **2012**, *13*, 312. [[CrossRef](#)] [[PubMed](#)]
67. Zhang, J.; Kobert, K.; Flouri, T.; Stamatakis, A. PEAR: A fast and accurate Illumina Paired-End reAd mergeR. *Bioinformatics* **2014**, *30*, 614–620. [[CrossRef](#)] [[PubMed](#)]
68. Haas, B.J.; Papanicolaou, A.; Yassour, M.; Grabherr, M.; Blood, P.D.; Bowden, J.; Couger, M.B.; Eccles, D.; Li, B.; Lieber, M.; et al. De novo transcript sequence reconstruction from RNA-seq using the Trinity platform for reference generation and analysis. *Nat. Protoc.* **2013**, *8*, 1494–1512. [[CrossRef](#)]
69. Fu, L.; Niu, B.; Zhu, Z.; Wu, S.; Li, W. CD-HIT: Accelerated for clustering the next-generation sequencing data. *Bioinformatics* **2012**, *28*, 3150–3152. [[CrossRef](#)]
70. Nachtigall, P.G.; Rautsaw, R.M.; Ellsworth, S.A.; Mason, A.J.; Rokyta, D.R.; Parkinson, C.L.; Junqueira-de Azevedo, I.L.M. ToxCodAn: A new toxin annotator and guide to venom gland transcriptomics. *Briefings Bioinform.* **2021**, *22*, bbab095. [[CrossRef](#)]
71. Li, H. Aligning sequence reads, clone sequences and assembly contigs with BWA-MEM. *arXiv* **2013**, arXiv:1303.3997. [[CrossRef](#)]
72. Rokyta, D.R.; Margres, M.J.; Ward, M.J.; Sanchez, E.E. The genetics of venom ontogeny in the eastern diamondback rattlesnake (*Crotalus adamanteus*). *PeerJ* **2017**, *5*, e3249. [[CrossRef](#)]

73. Li, B.; Dewey, C.N. RSEM: Accurate transcript quantification from RNA-Seq data with or without a reference genome. *BMC Bioinform.* **2011**, *12*, 323. [[CrossRef](#)]
74. Love, M.I.; Huber, W.; Anders, S. Moderated estimation of fold change and dispersion for RNA-seq data with DESeq2. *Genome Biol.* **2014**, *15*, 550. [[CrossRef](#)] [[PubMed](#)]

Disclaimer/Publisher’s Note: The statements, opinions and data contained in all publications are solely those of the individual author(s) and contributor(s) and not of MDPI and/or the editor(s). MDPI and/or the editor(s) disclaim responsibility for any injury to people or property resulting from any ideas, methods, instructions or products referred to in the content.